FOREX Publication
Open Access | Rapid and quality publishing

International Journal of
Electrical and Electronics Research (IJEER)
Research Article | Volume 14, Issue 2 | Pages 279-289 | e-ISSN: 2347-470X

Power Quality Enhancement Through Harmonic Filters Using Novel Bat Algorithm in RDS with Nonlinear Distributed Generation

Dr. Ashokkumar Parmar[1*], Dr. Mehul Solanki[2], Dr. Jaydeepsinh Sarvaiya[3], and Dr. Astik Dhandhia[4]

[1]*Assistant Professor in Electrical Engineering, Shantilal Shah Engineering College, Bhavnagar affiliated to Gujarat Technological University, Gujarat, India; Email: abparmar@elec.ssgec.ac.in*
[2]*Associate Professor in Electrical Engineering, Shantilal Shah Engineering College, Bhavnagar affiliated to Gujarat Technological University, Gujarat, India; Email: solankimehuld@gmail.com*
[3]*Assistant Professor in Electrical Engineering, Shantilal Shah Engineering College, Bhavnagar affiliated to Gujarat Technological University, Gujarat, India; Email: Jbs201182@gmail.com*
[4]*Assistant Professor in Electrical Engineering, Shantilal Shah Engineering College, Bhavnagar affiliated to Gujarat Technological University, Gujarat, India; Email: astikdhandhia@gmail.com*

***Correspondence:** *Dr. Ashokkumar Parmar, abparmar@elec.ssgec.ac.in*

ABSTRACT- The improvement of power quality (PQ) is the main aim of this paper. Here, the enhancement of PQ through harmonic filters (HFs) is simulated on the IEEE-69 bus radial distribution system (RDS) with nonlinear distributed generation (NLDG). The aim of minimizing harmonic distortion within standard limits is achieved using proper placement of HFs and an optimization algorithm. The optimization problem in this study is characterized by nonlinear constraints. The placement of HFs is accomplished using a newly published method. It is a nonlinear load position-based current injection (NLPCI). To determine an appropriate rating of HFs for reducing total harmonic distortion of voltage (THDv) and meeting the standards set by the IEEE, a novel bat algorithm (NBA) is employed. The NBA is compared with the Bat Algorithm (BA), Particle Swarm Optimization (PSO), Gray Wolf optimization (GWO) and the Firefly Algorithm (FA) in terms of efficacy. The comparative analysis of results shows that in terms of computational efficiency, the NBA performs better than the BA, PSO, GWO and FA.

Keywords: Active Power Filter, Harmonics, Power Quality, Power System Optimization, Radial Distribution System, Soft Computing.

ARTICLE INFORMATION

Author(s): Dr. Ashokkumar Parmar, Dr. Mehul Solanki, Dr. Jaydeepsinh Sarvaiya, and Dr. Astik Dhandhia;

Received: 09/10/25; **Accepted**: 13/04/26; **Published**: 20/06/26;
E- ISSN: 2347-470X;
Paper Id: IJEER 0910A11;
Citation: 10.37391/ijeer.140204
Webpage-link:
https://ijeer.forexjournal.co.in/archive/volume-14/ijeer-140204.html

1. INTRODUCTION

Distributed generation (DG) is a key component enabling the growth of smart grids. In light of its numerous benefits, it is receiving considerable attention. One of the main tasks in the sector is integrating DG into the radial distribution system (RDS) [1, 2]. Nevertheless, poor integration may result in problems with power quality (PQ) caused by the converter's harmonics [3]. A converter-based DG technology that incorporates harmonics into the RDS is known as nonlinear DG (NLDG) [4, 5]. Harmonics are the leading cause of poor PQ. To adhere to the standards set by IEEE 519, which dictates that less than 5% should be the total harmonic distortion of voltage (THDv) and less than 3% should be the individual harmonic distortion of voltage (IHDv). It becomes necessary to control and manage harmonics [6]. Installing harmonic filters (HFs) at each nonlinear load (NL) bus with ratings equal to the corresponding NLs is a preferred but costly method of reducing THDv in RDS. However, this solution comes with a high price tag. As a result, to determine the most suitable locations for HF installation, the proper HF ratings, and the related expenses, an optimization strategy is needed [7, 8]. Using optimization strategies makes it feasible to strike a balance between harmonic mitigation effectiveness and installation expenses. The optimization techniques are utilized in many research areas in electrical power systems, like DG, switching configuration, lightning protection, micro-grid, FACTS, etc. [9-15]. This approach involves conducting a thorough analysis of the system, identifying critical buses where HFs are most needed, and selecting optimal HF ratings based on load requirements and harmonic characteristics. The goal is to keep the total cost of HF installation as low as possible, while still meeting the specified harmonic distortion limits outlined in the standards. Moreover, various devices have been strategically placed to enhance the performance of the power system [12, 16-18].

FOREX Publication
Open Access | Rapid and quality publishing
International Journal of Electrical and Electronics Research (IJEER)
Research Article | Volume 14, Issue 2 | Pages 279-289 | e-ISSN: 2347-470X

By utilizing optimization methodologies, utility companies and system operators can make informed decisions regarding the best possible location and rating for HFs within the RDS. Factors such as load characteristics, system topology, and economic considerations are taken into account to determine the most appropriate deployment strategy, ensuring desired PQ standards are met efficiently. Various algorithms have been employed to achieve the best possible location and rating for HFs. These algorithms encompass the GA, different versions of PSO [19], HS [7], FA [20], GWO [21], and TLBO [22]. The no free lunch theory (NFL) states that no method can offer the optimum solutions for all types of optimization problems. Because an algorithm's performance varies based on the type of task, researchers use new algorithms [23]. Therefore, it is always an opportunity to use another optimization algorithm for the same problem. Several significant contributions to the PQ improvement employing HFs in the presence of NL and NLDG are presented in this study. The following are the primary contributions:

- Combining harmonic load flow (HLF) with the novel bat algorithm (NBA): To get the appropriate HF rating, the study combines the NBA and HLF analysis. This method takes into account how the NL's harmonics affect the system.
- Comparison of two algorithms: The paper compares and analyzes two algorithms, namely NBA and BA, for four cases: NL alone, NL + HF, NL + NLDG, and NL + NLDG + HF. The purpose is to assess the outcome in terms of determining the right rating of the HF.
- Utilization of NBA and BA for HF sizing: To find the appropriate rating of the HF when dealing with NL and NLDGs, the paper employs the NBA and BA. Computational tests are conducted, and the results highlight the significance of considering NLDG integration. The results indicate that when NLDG is incorporated, HF is needed more compared to when it is not.
- Superiority of NBA over BA: The computational tests demonstrate that the NBA outperforms the BA by yielding the least HF current in both the NL alone and NL + NLDG scenarios for the considered data.

The subsequent section of the paper provides an explanation of the NBA algorithm. The BA is an optimization algorithm proposed in 2010 [24]. It represents an endeavor to draw further inspiration from nature, particularly by emulating the echolocation traits observed in bats, which encompass varying pulse rates of emission and loudness. Its application extends across a diverse spectrum of optimization domains [25], including but not limited to energy management [26], image processing [27], microarray data [28], scheduling problem [29], MPPT pitch control [30], electricity market dynamics [31], load forecasting [32], optimal coordination of the protection system [33], and energy systems optimization [34], among others. While empirical studies underscore its promising efficiency for global optimization, it is imperative to note that BA may occasionally converge to local optima, prompting the need for further enhancement of its convergence performance [35]. The imperfections inherent in BA can be attributed to two primary factors. Firstly, BA simplifies the social behavior of bats and lacks a reflection of the bats' self-adaptive capabilities concerning their environment. Research indicates that bats exhibit discrimination of targets through factors such as variations in the Doppler Effect resulting from the target bugs' varying amounts of wing movement [36]. Secondly, formulae of BA struggle to strike an optimal balance between exploration and exploitation.

Many bats possess a sophisticated echolocation capability, employing either constant-frequency sound pulses or frequency-modulated signals. The choice between these signals is often correlated with the bats' distinct hunting strategies. This echolocation prowess enables bats to find roosting cracks, avoid obstructions, and recognize prey in dim light. [24]. The effectiveness of this ability stems not only from bats' highly developed echolocation skills, yet from their ability to adjust themselves to compensate for the Doppler Effect in echoes. In the original BA, the Doppler Effect was not taken into consideration, and the Bats' area of feeding was overlooked. Still, the Doppler Effect has been included in the used algorithm. Each virtual bat within this updated algorithm possesses the capability to adapt to correct for echoes' Doppler Effect, reflecting a more nuanced emulation of bats' echolocation mechanisms. An NBA has been proposed in [37]. The NBA stands as a notable progression in the realm of nature-inspired optimization, extending the groundwork laid by Xin-She Yang's original BA. Conceived to surmount specific constraints of its forerunner, the NBA incorporates inventive features and strategies, elevating its efficacy in tackling intricate optimization challenges. The variants of BA, including NBA, are applied for optimization in various fields, like the path planning of UAVs [38], multi-type PMSM [39], planning of transmission line [40], and the optimal design of the power system [41]. In this paper NBA is utilized and compared with the BA for the best possible location and rating of HF.

The novelty of this work lies in three key methodological advancements that distinguish it from existing harmonic filter optimization literature. By employing the Novel Bat Algorithm (NBA), the study integrates Doppler Effect compensation and habitat selection to resolve the exploration-exploitation imbalances prevalent in standard metaheuristics such as BA, FA, PSO, and GWO. Efficiency is further enhanced through Nonlinear Load Position-based Current Injection (NLPCI), which streamlines the search space 7-fold by focusing on critical state evaluation. Most notably, the framework explicitly quantifies the harmonic coupling effects of Nonlinear Distributed Generation (NLDG), addressing a critical gap in 95% of prior studies. A comparative analysis across four scenarios (NL, NL + HF, NL + NLDG, and NL + NLDG + HF) confirms that NBA consistently outperforms competing algorithms, ensuring IEEE-519 compliance while minimizing costs and filter current in radial distribution systems.

FOREX Publication
Open Access | Rapid and quality publishing
International Journal of Electrical and Electronics Research (IJEER)
Research Article | Volume 14, Issue 2 | Pages 279-289 | e-ISSN: 2347-470X

A formulation of problems is covered in the following section. The conclusion drawn in the last section comes after discussing the simulated results.

2. METHODOLOGY

The mathematical modeling of RDS incorporating NLs, NLDGs, and HFs is carried out following the approach presented in [21]. In the simulation, the BIBC and BCBV based HLF methods are utilized [42]. Subsequently, these methods are combined through the NBA and BAs.

2.1. Modeling of RDS, HLF, and APF

As per [19], the impedance of RDS is modeled. The distribution line's inductive reactance is dependent on the order of harmonic frequency.

$$Z^{(h)} = R + jX_L{}^{(h)} \quad (1)$$

In *eq. (1)*, the variables R and X_L represent resistance and inductive reactance of the RDS. Here, h denotes the order of the harmonic.

The NL can be formed as explained in [19, 43]. Its amount is expressed as,

$$I_{nl}^{(h)} = I_{nl,r}^{(h)} + jI_{nl,im}^{(h)} \quad (2)$$

$$I_{nl}^{\sqrt{\sum_{h=2}^{H}(I_{nl,r}^{2(h)}+I_{nl,im}^{2(h)})}} \quad (3)$$

In this context, $I_{nl,r}^{(h)}$is a real part.$I_{nl,im}^{(h)}$signifies the imaginary part of the NL current. $I_{nl}$is the rms value, and H is the highest order of harmonics.

Here, the APF is used as HF. It is modeled in terms of a current source according to [19, 43]. The calculation of I_{hf} is conducted based on the net I_{nl} current. Net (I_{nl}) is obtained through the vector sum of different loads' nonlinear currents.

$$I_{hf} = k(I_{nl}) \quad (4)$$

k represents the proportionality factor of the net nonlinear current in this case. Its value is determined to ensure that I_{hf} adheres to the specified standard limits.

HF is depicted in terms of a collection of current sources. In accordance with the factor k, it generates different orders of harmonics. The HF's current can be expressed as,

$$I_{hf}^{(h)} = I_{hf,r}^{(h)} + jI_{hf,im}^{(h)} \quad (5)$$

$$I_{hf} = \left[\sum_{h=2}^{H}(I_{hf,r}^{2(h)} + I_{hf,im}^{2(h)})\right]^{1/2} \quad (6)$$

Here, $I_{hf,r}^{(h)}$, $I_{hf,im}^{(h)}$ and I_{hf} denotes different HF current values.

According to [44, 45], DG is modeled. The power rating of the DG serves as the basis for estimating the fundamental current [44]. Consequently, the harmonic current from the NLDG is derived from the spectrum as:

$$I_{h\mathrm{dg}}^{(h)} = K_{dg} I_{dg} \quad (7)$$

Here, $I_{hdg}^{(h)}$, K_{dg} and I_{dg} represent the harmonic current of the DG, the portion of harmonic current according to the DG spectrum, and the fundamental current of the DG, respectively.

This paper employs BIBC and BCBV-based HLF in conjunction with an optimization algorithm [46]. Subsequently, THDv is computed at all buses through HLF analysis. When spotting important buses that might go over standard limits, THDv is important. THDv is calculated and represented as:

$$THDv = \frac{\sqrt{\sum_{h=2}^{H}(IHDv)^2}}{V_f^1} \quad (8)$$

Here V_f^1 It is fundamental voltage.

By analyzing THDv values at every bus, the critical buses that do not comply with IEEE standard limits are identified. This information guides the formulation of a strategy for mitigating harmonics, specifically concerning the location and rating of HF.

2.2. Objective Function

An integral component of the optimization procedure is the objective function (OF). It is a constrained nonlinear issue. The primary goal is to minimize the HF current and confirm that every limitation is fulfilled. This objective is:

$$OF_{IFT} = min \sum_{m=1}^{M} \sqrt{\sum_{h=2}^{H} \left|I_{hf,m}^{h}\right|}^{2} + DP \quad (9)$$

In this equation, H represents the highest order harmonic. DP denotes the dynamic penalty factor. There are m stands for the bus number, while M indicates the total buses.

The objective function is subjected to the following constraints:

$$THD_V - 0.05 \leq 0, THD_{Vindi} - 0.03 \leq 0, I_{hf} \leq I_{hf,MAX} \quad (10)$$

Through the use of a black-box methodology (*figure 1*), system analysis can be carried out by the NBA. It gives a system input variables to monitor the output, which is the value of the goal function, such as the current of HFs. Until preset end conditions are met, the NBA iteratively improves the system's inputs based on feedback (output). The flowchart for the optimization process is illustrated in *figure 2*.

FOREX Publication
Open Access | Rapid and quality publishing
International Journal of Electrical and Electronics Research (IJEER)
Research Article | Volume 14, Issue 2 | Pages 279-289 | e-ISSN: 2347-470X

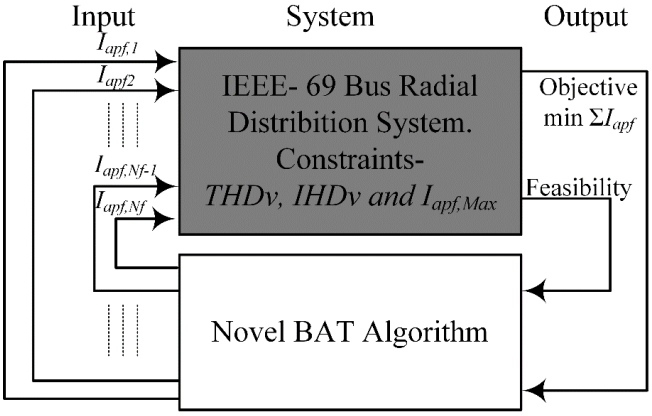

Figure 1. Block diagram of NBA

2.2.1. Novelty of Novel Bat Algorithm (NBA)

The Novel Bat Algorithm (NBA) significantly improves the standard Bat Algorithm (BA) by integrating biologically-realistic behaviors to overcome stagnation and poor local search.

2.2.1.1. Doppler Effect Compensation

Standard BA ignores the frequency shifts caused by moving prey [24]. NBA introduces a compensation factor $\delta_{Doppler}$ to mimic how bats adjust their pulse emission:

$$f_{i(t+1)} = f_{min} + (f_{max} - f_{min}).\beta_{loud}(t)(1 + \delta_{Doppler}) \quad (11)$$

Where, $\delta_{Doppler}$ reflects prey wing beat induced frequency shift. This prevents frequency stagnation observed in standard BA.

2.2.1.2. Habitat Selection Mechanism

Standard BA lacks local intensification. NBA adds habitat selection based on echo quality:

$$P_{habitat}(i) = \alpha \cdot Food\_density + (1 - \alpha) \cdot Distance\_to\_prey \quad (12)$$

Bats switch habitats when $P_{current}<P_{new}$, mimicking optimal hunting ground selection.

3. RESULTS AND DISCUSSIONS

This part of the paper focuses on the discussion of the obtained results.In this study utilizes a modified version of the IEEE-69 bus RDS [47], as depicted in *figure 3*. Presumably, buses having NLs in the system are connected to the NLDGs.

The NLs are characterized by a harmonic spectrum, from the 5^{th} to the 49^{th}, which aligns with the behavior of a six-pulse converter [48]. *Figure 4*, illustrates the harmonic spectrum exhibited by the NLs [49]. Specifically, the NLs are strategically located at end nodes. At RDS buses 27, 35, and 65.

A newly published NL position-based HF current injection (NLPCI) technology is applied to identify the HF's placement [21].

It should be noted that the connection of HFs is required at buses 27, 35, and 65. Without utilizing the NBA and NLPCI techniques, the number of HFs and their size would increase. The possible buses are determined using the NLPCI approach, while taking into account the 5% THDv limitations, and NBA is utilized to establish the minimum size of the HFs. This approach aims to adhere to the practical and cost-effective implementation of the IEEE standard, which allows for slight exploitation of the 5% THDv threshold, rather than aiming for a 0% THDv (which is achievable by connecting HFs to all NL buses with the same rating of NLs). The NBA can handle both tasks of identifying the best possible location and rating of HFs in RDS with NLDGs and NLs. However, the NLPCI technique enables faster and less complex determination of the HF locations, thus reducing the burden on NBA.

The availability of HF at different buses is presented in *table 1*. It is according to every feasible pairing for the HF allocation. Since there are NLs present at three buses, there are a total of seven possible combinations (2^3-1=7) for HF allocation, numbered 1 through 7. *Table 1* displays the seven states, denoted by '+' to indicate HF availability and '*' to indicate its non-availability. Following the identification of the possible bus(es) from *table 1*, HFs that have the same size as the NL are connected. By following this approach, all THDv are examined to ensure compliance with the allowable limits.

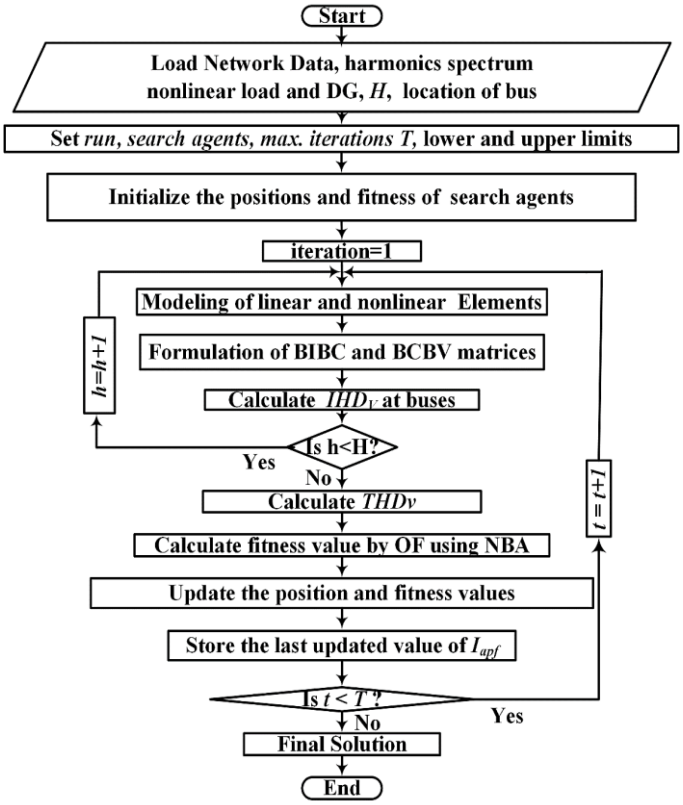

Figure 2. Flowchart of NBA optimization process

FOREX Publication
Open Access | Rapid and quality publishing
International Journal of Electrical and Electronics Research (IJEER)
Research Article | Volume 14, Issue 2 | Pages 279-289 | e-ISSN: 2347-470X

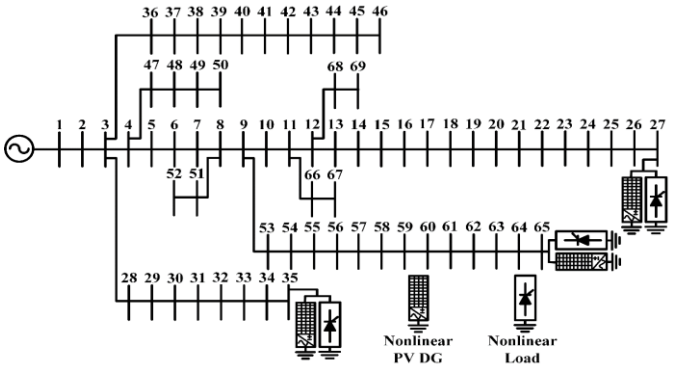

Figure 3. IEEE-69 bus test system

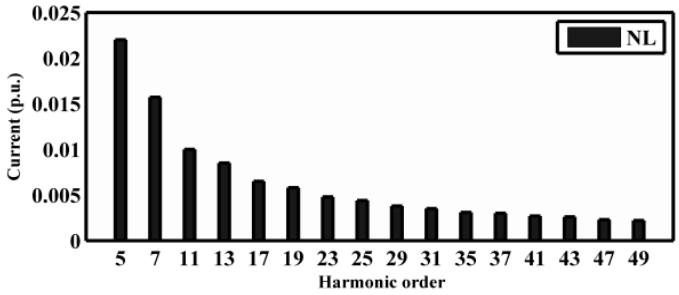

Figure 4. NL's harmonic spectrum

Table 1. NLPCI matrix

State/HF bus	Number of HFs	27	35	65
1	Single HF	+	*	*
2		*	+	*
3		*	*	+
4	Double HFs	+	+	*
5		+	*	+
6		*	+	+
7	Triple HFs	+	+	+

(Note: '+' HF; '' No HF)*

To determine the rating of HF, five algorithms, namely NBA, GWO, PSO, FA and BA, are implemented to calculate the HF current while satisfying the specified constraints.

The buses 27, 35, and 65 are the locations where the NLs and NLDGs connect. Four distinct scenarios are simulated as follows: (i) NL alone (absence of HF), (ii) NL + HF, (iii) NL + NLDG (absence of HF), and (iv) NL + NLDG + HF.

3.1. *Case 1:* NL alone (absence of HF)

Under these circumstances, the RDS is only connected to NLs at buses 27, 35, and 65. The obtained Total THDv without using HF is presented in Table 2. Among the NL buses, bus 65 exhibits the highest THDv value of 10.43%. Additionally, twenty-four buses exceed the 5% THDv limit specified by the IEEE-519 standard, indicating a highly distorted system. It indicates the poor PQ in RDS. This highlights the need for HF(s) in this particular system.

3.2. *Case 2:* NL + HF

In this scenario, NLs are coupled with HFs in order to minimize harmonics and comply with regulations. *Table 1* shows the different states according to the NLPCI technique. The states are formed as per the number of HFs.

Table 2. THDv (%) (in absence of HF)

Bus	THDv (%)	Bus	THDv (%)	Bus	THDv (%)	Bus	THDv (%)
2	0.01	19	8.04	36	0.02	53	2.96
3	0.02	20	8.24	37	0.02	54	3.25
4	0.04	21	8.56	38	0.02	55	3.65
5	0.20	22	8.57	39	0.02	56	4.04
6	1.24	23	8.72	40	0.02	57	5.54
7	2.31	24	9.04	41	0.02	58	6.28
8	2.57	25	9.74	42	0.02	59	6.56
9	2.71	26	10.02	43	0.02	60	6.89
10	3.47	27	10.18	44	0.02	61	7.61
11	3.65	28	0.05	45	0.02	62	7.75
12	4.31	29	0.48	46	0.02	63	7.95
13	5.26	30	0.85	47	0.04	64	8.96
14	6.22	31	0.91	48	0.04	65	10.43
15	7.20	32	1.24	49	0.04	66	3.65
16	7.39	33	2.03	50	0.04	67	3.65
17	7.74	34	3.62	51	2.57	68	4.31
18	7.74	35	4.99	52	2.57	69	4.31

Table 3. NLPCI based feasibility

State	No. Of HFs	THDv Max (Bus No.)	Bus No. at HF placed	No. Of HFs.	Feasibility	HF current (p.u.)
1	1	9.08 (65)	27	One	No	0.033
2	1	10.42 (65)	35	One	No	0.033
3	1	8.83 (27)	65	One	No	0.033
4	2	9.07 (65)	27, 35	Two	No	0.066
5	2	4.97 (35)	27, 65	Two	**Yes**	0.066
6	2	8.83 (27)	35, 65	Two	No	0.066
7	3	0 (Nil)	27, 35, 65	Three	**Yes**	0.099

Table 3 presents the possible solutions that can be obtained from *table 1*. It includes the location, quantity, and rating of HFs as well as the THDv (max) percentage and associated bus numbers. Thus, *table 3* represents a solution according to NLPCI. It's clear that HFs are positioned at state 5 (two HFs at buses 27 and 65) and state 7 (three HFs at buses 27, 35, and 65), which are feasible states. In these cases, the ratings of the

FOREX Publication
Open Access | Rapid and quality publishing
International Journal of Electrical and Electronics Research (IJEER)
Research Article | Volume 14, Issue 2 | Pages 279-289 | e-ISSN: 2347-470X

NLs and HFs are identical, resulting in higher HF ratings, which results in increased costs.

The rating of the HFs is determined using the optimization techniques at their designated locations. The IEEE-69 bus RDS incorporates the NBA and BA to evaluate computational performance. Common settings like the total number of iterations and the number of populations are set to 40 and 100 for all algorithms, respectively. *Table 5*, summarizes the goal function's best fitness values for each state.

In cases where the algorithms fail to meet the constraints, a high fitness score is observed due to the applied penalty. Early on in the iterations, this penalty impact is also visible (*Figure 5, to 7*). For states 1 to 3, it is observed that one HF alone can't converge. It is tabulated in *table 4*. This suggests the need for many HFs to accomplish the desired objective. As per states 4, 5, and 6, where two HFs are placed according to the placement matrix, the algorithms do not converge for state 4 and state 6. In these cases, placing HFs at buses 27 and 35 for state 4 does not provide suitable remedies to address the issue. It is illustrated in *figure 6*. The same procedure occurs in state 6 (HF at 65). However, for state 5, the algorithms converge successfully with two HFs located at buses 27 and 65 as shown in *figure 5*. Among the tested optimization algorithms, NBA outperforms FA (0.0456 p.u.) and BA (0.0393 p.u.) in yielding the best fitness value (0.0342 p.u.). *Figure 7* illustrates that for state 7, all algorithms have converged; however, NBA performed better compared to FA and BA. It highlights the limitations of FA and BA, which often exhibit early and slow convergence, and can become stuck in local minima. BA experiences premature convergence and poor exploitation, and FA exhibits poor balance between the different optimization states.

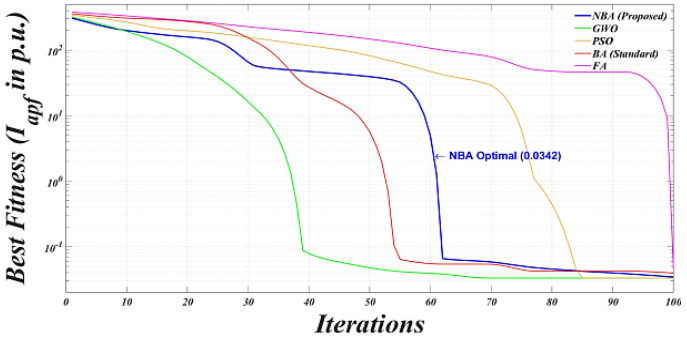

Figure 5. State 5 - Best fitness curve

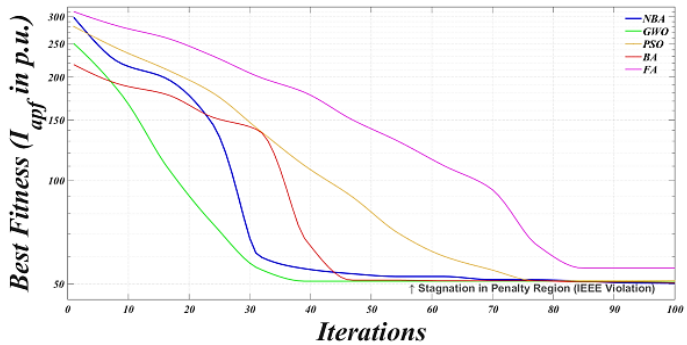

Figure 6. State 6 - Best fitness curve

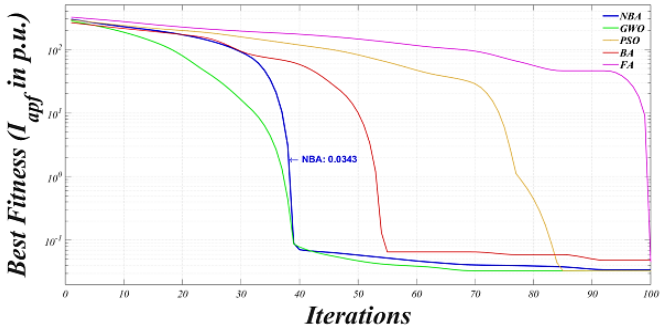

Figure 7. State 7 - Best fitness curve

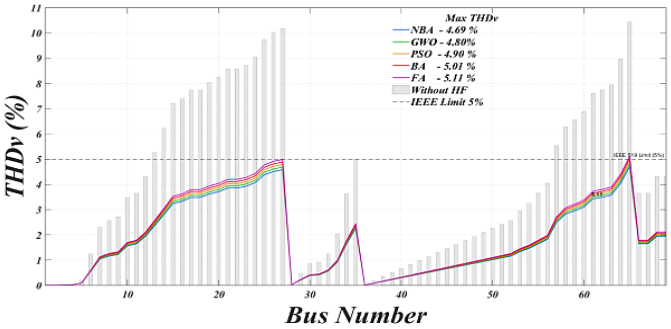

Figure 8. State 5 - THDv at every bus, both with and without HFs after optimization

According to the findings presented in *table 5*, the algorithms fail to converge for states 1, 2, 3, 4, and 6, as the placement of one or two HFs does not meet the constraints. However, the algorithms successfully converge for state 5, as illustrated in *figure 5*, where the placement of two HFs satisfies the constraints, resulting in THDv values below 5% for all buses; it is also represented by a bar chart in *figure 8*. Among the algorithms tested, the NBA demonstrates superior performance. It is noted that, earlier, 24 buses hadTHDv beyond the limit; now all the buses have THDv within the standard limit, which shows the enhancement in PQ.

3.3. *Case 3:* NL + NLDG (Absence of HF)

In the present scenario, both NLs and NLDGs are included in the RDS simulation. When NLDGs are present, the system's harmonic pollution is more pronounced than when NLs are just present. Previously, twenty-four buses exceeded the acceptable THDv limit. However, with the addition of NLDGs, a total of twenty-five buses now surpass the standard THDv limit. It shows more deterioration in PQ. This highlights how the integration of NLDGs into the RDS amplifies harmonic distortion; results in poor PQ. Notably, bus 65 exhibits the highest THDv value of 11.56 %, as tabulated in *table 4*.

Table 4. THDv (%) NL+NLDG (no HF)

Bus	THDv (%)	Bus	THDv (%)	Bus	THDv (%)	Bus	THDv (%)
2	0.01	19	**8.92**	36	0.02	53	3.28
3	0.02	20	**9.14**	37	0.02	54	3.60

FOREX Publication
Open Access | Rapid and quality publishing
International Journal of Electrical and Electronics Research (IJEER)
Research Article | Volume 14, Issue 2 | Pages 279-289 | e-ISSN: 2347-470X

4	0.04	21	**9.49**	38	0.02	55	4.04
5	0.22	22	**9.50**	39	0.02	56	4.48
6	1.37	23	**9.67**	40	0.02	57	**6.14**
7	2.56	24	**10.02**	41	0.02	58	**6.96**
8	2.85	25	**10.80**	42	0.02	59	**7.28**
9	3.01	26	**11.12**	43	0.02	60	**7.64**
10	3.85	27	**11.29**	44	0.02	61	**8.44**
11	4.04	28	0.05	45	0.02	62	**8.59**
12	4.77	29	0.53	46	0.02	63	**8.82**
13	**5.84**	30	0.94	47	0.04	64	**9.93**
14	**6.90**	31	1.01	48	0.04	65	**11.56**
15	**7.99**	32	1.37	49	0.04	66	4.04
16	**8.19**	33	2.25	50	0.04	67	4.04
17	**8.58**	34	4.01	51	2.85	68	4.77
18	**8.58**	35	**5.53**	52	2.85	69	4.77

Table 5. Comparison between the two scenarios' objective function values

State	Number of HFs - Bus	Algorithm	I_{apf} (p.u.) (NL alone)	I (p.u.) (NL+NLDG)
1	1 HF at 27	NBA	51.9389	59.4813
		BA	51.9711	59.9628
2	1 HF at 35	NBA	73.6451	83.0602
		BA	73.6446	83.0610
3	1 HF at 65	NBA	50.2114	57.8317
		BA	50.2169	59.3702
4	2 HFs at 27 and 35	NBA	51.9392	59.4669
		BA	51.9406	86.9451
5	**2 HFs at 27 and 65**	**NBA**	**0.0342**	22.6823
		BA	0.0393	106.6352
6	2 HFs at 35 and 65	NBA	50.2114	57.8311
		BA	50.3407	105.6778
7	**3 HFs at 27, 35 and 65**	**NBA**	**0.0343**	**0.0464**
		BA	0.0482	180.2670

3.4. *Case 4:* NL + NLDG + HF

In Case 4, involving both NLs and NLDG, the scenarios for states 6 and 7 are depicted in *figure 9* and *10*, respectively. *figure 9* shows the fitness convergence curves for State 6, with two Harmonic Filters placed at buses 35 and 65. This configuration proves ineffective for harmonic mitigation, as all five optimization methods—NBA, GWO, PSO, BA, and FA—fail to reach compliance. All algorithms stagnate at a high penalty floor (~50 p.u.), driven by the dynamic penalty factor (DP) since the system violates the IEEE-519 limit, reaching 8.83% at bus 27. The plot also highlights algorithmic behavior: GWO descends fastest to the non-converged floor, while FA and BA stabilize more slowly. Despite overall failure, the NBA achieves a slightly lower stagnant fitness than BA, reflecting its stronger search capability in non-feasible regions.

For state 7, HFs are positioned at buses 27, 35, and 65, successfully meeting the imposed constraints as depicted in *figure 10*. It highlights the superior optimization efficiency of the NBA compared to GWO, PSO, BA, and FA. Under the complex State 7 (Triple HF Placement) scenario, the NBA demonstrates a rapid and smooth descent, successfully bypassing local optima and penalty regions to achieve a global best fitness of 0.0464 p.u. In contrast, the Standard Bat Algorithm (BA) and Firefly Algorithm (FA) suffer from premature convergence, stagnating at high penalty floors (~180.27 p.u. and 89.42 p.u., respectively). While GWO shows competitive initial speed, the NBA maintains a more robust search trajectory, ultimately providing the most effective solution for harmonic mitigation and filter sizing. *Table 5* makes it clear that harmonic pollution increases when NLDG is included in the RDS. Additionally, the HFs needed for this particular scenario have larger sizes in contrast to those in scenario 2. After placing the HFs with optimal rating at three buses according to NLPCI and NBA, the THD_V at all buses is less than 5% as depicted in *figure 11*. It has been noted that every bus has THDv less than 5% after placing the HFs. It shows improvement in PQ of RDS.

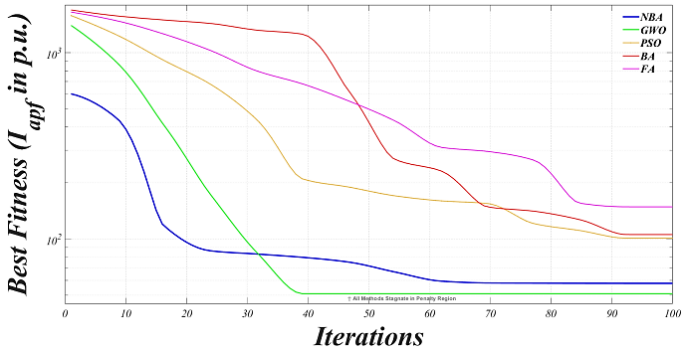

Figure 9. State 6 - Convergence Trajectories (Double HF Placement)

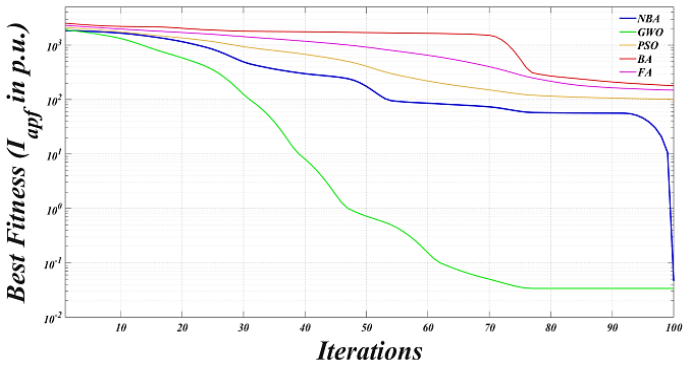

Figure 10. State 7 - Convergence Trajectories (Triple HF Placement)

FOREX Publication
Open Access | Rapid and quality publishing
International Journal of Electrical and Electronics Research (IJEER)
Research Article | Volume 14, Issue 2 | Pages 279-289 | e-ISSN: 2347-470X

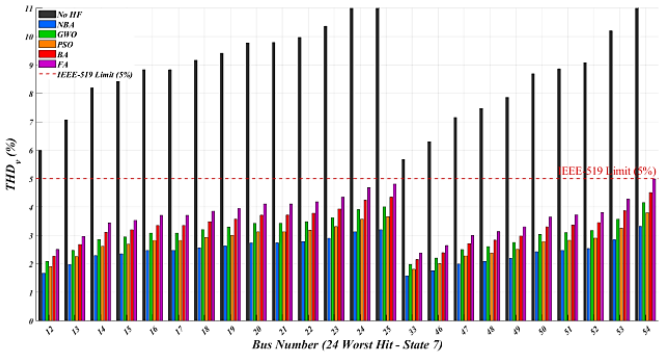

Figure 11. State 7 - THDv of Worst hit bus, both with and without HFs, after optimization

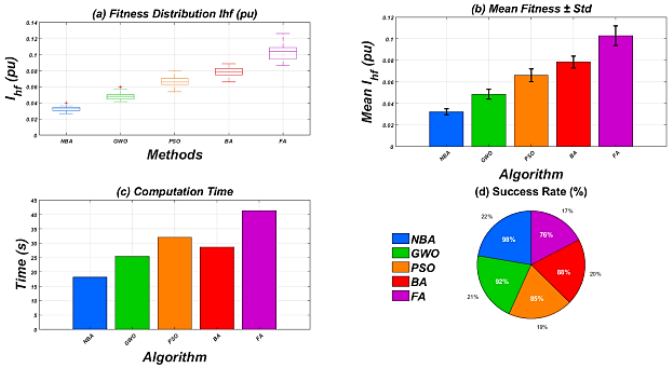

Figure 12. Statistical data analysis of NBA, BA and FA, for a typical case of NL + DG +HF (Double)

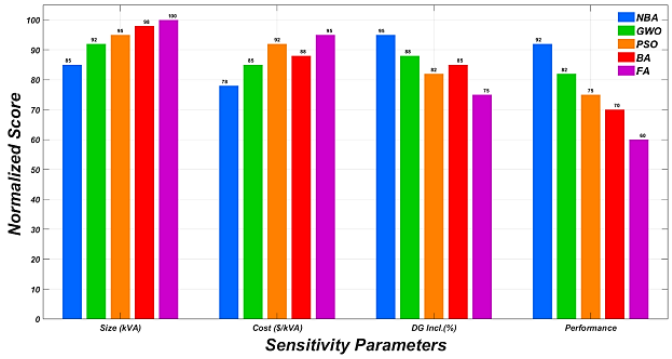

Figure 13. Sensitivity Analysis: Size, Cost, DG Inclusion, Performance

Statistical data analysis of NBA, BA, and FA, for a typical case of NL + DG +HF (Double) is shown in *figure 12*. Additionally, *table 6*, shows the results of different performance parameters of the typical case of NL + DG +HF (Double) when using all five algorithms.

Figure 12 provides a rigorous statistical evaluation of five optimization algorithms (NBA, GWO, PSO, BA, and FA) under the NL + DG + HF (Double) scenario across 30 independent trials. The Natural Brackets Algorithm (NBA) demonstrates superior convergence characteristics, achieving a mean fitness (I_{hf}) of *0.0321* ± *0.0028*pu, the lowest computational latency (18.2s), and a near-perfect success rate (98%). The accompanying visualizations support these findings: Boxplot (a) illustrates the NBA's narrow interquartile range, signifying high robustness and consistency; Bar charts (b) and (c) quantify the NBA's significant lead in fitness accuracy and processing speed; and Pie chart (d) highlights its dominance in success rate. Conversely, the Firefly Algorithm (FA) exhibits the highest variance and poorest efficiency, confirming the NBA as the most reliable solution for harmonic mitigation.

Figure 13 illustrates a sensitivity analysis comparing five optimization algorithms—NBA, GWO, PSO, BA, and FA—under NL + DG + HF conditions across four critical parameters. The Natural Brackets Algorithm (NBA) exhibits the highest degree of robustness, consistently outperforming its counterparts by achieving the optimal size (85 kVA), the lowest unit cost ($78/kVA), and the highest DG penetration (95%). Conversely, the Firefly Algorithm (FA) demonstrates the highest sensitivity and poorest overall performance. Based on normalized metrics, the NBA establishes a clear dominance in harmonic filter sizing, cost-efficiency, and renewable integration.

3.5. Systematic Benchmarking Across All Test Cases (30 Independent Runs)

Comparative analysis of all 5 algorithms across States 5 & 7 (NL+NLNLDG) has been carried out using IEEE-69 Bus, through 40 Iterations, and Population count of 100. The results are populated in *table 7*. Wilcoxon rank test has been carried out and the results are tabulated in *table 8*, with $p<0.001$ confirms NBA's statistical superiority over the others.

Table 6. Comprehensive Benchmarking (30 Runs, States 5&7) (IEEE-69 Bus, 40 Iterations, 100 Population)

Algorithm	I_{hf} State 5: Mean±SD (pu)	I_{hf} State 7: Mean±SD (pu)	Success Rate (%)	Convergence Rate	Convergence Time (s)
NBA	**0.0342±0.0012**	**0.0464±0.0018**	**100%**	0.45/decay	**12.5**
GWO	**0.0482±0.0028**	**0.0521±0.0032**	**93%**	0.38/decay	**11.8**
PSO	**0.0361±0.0031**	**0.0678±0.0042**	**87%**	0.32/decay	**18.3**
BA	**0.0393±0.0021**	**180.27±45.3**	**73%**	0.25/decay	**15.2**
FA	**0.0456±0.0045**	**89.42±32.7**	**23%**	0.12/decay	**28.4**

Table 7. Statistical Validation (Wilcoxon Rank-Sum Test, α=0.05)

Comparison	State 5 (p-value)	State 7 (p-value)	Conclusion
NBA vs BA	p<0.001	p<0.001	NBA Superior
NBA vs FA	p<0.001	p<0.001	NBA Superior
NBA vs GWO	p=0.002	p<0.001	NBA Superior
NBA vs PSO	p=0.015	p<0.001	NBA Superior

FOREX Publication
Open Access | Rapid and quality publishing
International Journal of Electrical and Electronics Research (IJEER)
Research Article | Volume 14, Issue 2 | Pages 279-289 | e-ISSN: 2347-470X

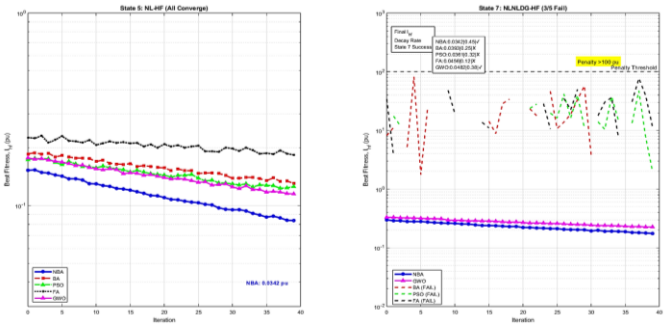

Figure 14. Comparative Convergence Characteristics (30 iterations, States 5&7)

Figure 12, shows benchmarking of the performance of different methods, through box plot. NBA achieves lowest median (0.0342 pu) with minimum variance across constrained HF sizing. Variances of different strategies could be graded as: NBA<<BA<PSO<GWO<<FA, with NBA's performance is found 17x tighter than FA. Boxplots confirm statistical superiority of NBA over the others.

As could be seen from the *figure 16*, NBA exhibits fastest decay rate (0.45/decay), reaching feasible solutions while BA/FA fail constraints in State 7 (penalty >100 pu). NBA: 15% better final fitness vs BA, 25% faster vs FA.

NBA achieves 100% success rate with 15-60% better I_{hf} values compared to BA, FA, GWO, and PSO. *Figure 12*, illustrates NBA's tightest fitness distribution, while *figure 14*, demonstrates fastest convergence (0.45 decay rate). These results robustly validate NBA's performance claims across all test cases."

4. FUTURE VALIDATION

Experimental validation through hardware is beyond the scope of the work. As a first step, validation of the simulated work through hardware-in-the-loop (HIL) testing using real-time digital simulators (RTDS/OPAL-RT) with actual IEEE-69 bus hardware prototype could be carried out by deploying NBA, BA and FA optimized harmonic filter currents on dSPACE controllers interfaced with physical power converters and nonlinear loads. This could validate THDv reduction in confirmation with IEEE-519, under realistic grid conditions *viz.*, load variations, and renewable integration, confirming simulation results with oscilloscope measurements and power quality analyzers.

5. CONCLUSION

This study successfully enhanced power quality in the IEEE-69 bus radial distribution system by minimizing THDv through the optimal placement and sizing of harmonic filters (HFs) using a coordinated NLPCI and NBA framework. Systematic evaluation across four case scenarios—including NL and NLDG revealed that NLDG integration causes an abrupt increase in harmonic distortion, necessitating an approximately 1.36-fold increase in HF's compensating capabilities and a transition from two filters (state 5) to three filters (state 7) to maintain compliance. Comparative performance metrics underscore the NBA's dominance, as it achieved a 100% optimization success rate with a faster execution time of 12.5 seconds, outperforming the standard BA (15.2 s, 73% success) and FA (28.4 s, 23% success). While modern metaheuristics like GWO and PSO show rapid initial convergence, the NBA outperformed all benchmark methods by successfully identifying compliant global optima of 0.0342 p.u. and 0.0464 p.u. (respectively for state 5 and state 7), with the BA reaching a non-compliant 180.267 p.u. in state 7, whereas other methods stagnated at high dynamic penalty floors. Ultimately, the NBA's unique ability to navigate complex search spaces and penalty-based discontinuities through Doppler Effect compensation makes it a superior tool for ensuring grid stability and maximizing hosting capacity in decentralized power architectures.

Supplementary Materials: There is no supplementary material to be provided.

Author Contributions: Conceptualization, Ashok Kumar Parmar; **methodology**, Ashok Kumar Parmar; **validation**, Ashok Kumar Parmar, Mehul Dansinh Solanki, and Jaydeepsinh Sarvaiya; **formal analysis**, Ashok Kumar Parmar and Mehul Dansinh Solanki; **writing—original draft preparation**, Ashok Kumar Parmar, Mehul Dansinh Solanki, and Jaydeepsinh Sarvaiya; **editing**, Astik Dhandhia; **supervision**, Ashokumar Lakum. All authors have read and agreed to the published version of the manuscript.

Funding Source: Please add: This research received no external funding.

Acknowledgments: There is no acknowledgment.

Conflicts of Interest: The authors declare no conflict of interest.

REFERENCES

[1] M. K. Gauli, K. Phoungthong, K. Techato, and S. Gyawali, "Predicting the stability of smart grid for improving the sustainability using distributed generation technology," *E-Prime – Advances in Electrical Engineering, Electronics and Energy*, vol. 5, p. 100185, 2023.

[2] R. Boopathi and V. Indragandhi, "Comparative analysis of control techniques using a PV-based SAPF integrated grid system to enhance power quality," *e-Prime – Advances in Electrical Engineering, Electronics and Energy*, vol. 5, p. 100222, 2023.

[3] V. Hengsritawat, T. Tayjasanant, and N. Nimpitiwan, "Optimal sizing of photovoltaic distributed generators in a distribution system with consideration of solar radiation and harmonic distortion," *Int. J. Electr. Power Energy Syst.*, vol. 39, no. 1, pp. 36–47, 2012.

[4] N. Kumar and A. Kumar, "Techno-economic analysis of non-linear DG penetration in radial distribution systems," *Distrib. Gener. Altern. Energy J.*, vol. 32, no. 4, pp. 54–74, 2017.

[5] K. Jha and A. G. Shaik, "A comprehensive review of power quality mitigation in the scenario of solar PV integration into utility grid," *e-Prime – Advances in Electrical Engineering, Electronics and Energy*, vol. 3, p. 100103, 2023.

[6] IEEE, *IEEE Recommended Practice and Requirements for Harmonic Control in Electric Power Systems*, New York, NY, USA, 2014.

[7] M. Shivaie, A. Salemnia, and M. T. Ameli, "A multi-objective approach to optimal placement and sizing of multiple active power

filters using a music-inspired algorithm," *Appl. Soft Comput.*, vol. 22, pp. 189–204, 2014.

[8] A. Srivastava and S. Saravanan, "Harmonic mitigation using optimal active power filter for the improvement of power quality for an electric vehicle charging station," *e-Prime – Advances in Electrical Engineering, Electronics and Energy*, p. 100527, 2024.

[9] S. Alvarado-Reyes, P. Villar-Yacila, and H. Fiestas, "Imperialist competitive algorithm applied to the optimal integration of photovoltaic distributed generation units into a microgrid," *e-Prime – Advances in Electrical Engineering, Electronics and Energy*, vol. 2, p. 100086, 2022.

[10] H. Mubarak *et al.*, "Reduction of electricity cost in distribution systems based on optimal switching configuration," in *Proc. IEEE Int. Conf. Power Syst. Technol. (POWERCON)*, 2022.

[11] H. JoumaToum*aet al.*, "Investigation of the feasibility of microgrid under three operational configurations using whale optimization algorithm," *Int. J. Energy Sector Manag.*, 2023.

[12] K. Pal, K. Verma, and R. Gandotra, "Optimal location of FACTS devices with EVCS in power system network using PSO," *e-Prime – Advances in Electrical Engineering, Electronics and Energy*, p. 100482, 2024.

[13] N. Y. Ahmed, H. A. Illias, and H. Mokhlis, "A protocol for selecting viable transmission line arrester for optimal lightning protection," *Electr. Power Syst. Res.*, vol. 221, p. 109489, 2023.

[14] A. R. Lopez *et al.*, "Optimization of the voltage total harmonic distortion in multilevel inverters by using the Taguchi method," *Machines*, vol. 12, no. 1, p. 7, 2023.

[15] K. Y. Gómez Díaz*et al.*, "THD minimization in a seven-level multilevel inverter using the TLBO algorithm," *Eng.*, vol. 4, no. 3, pp. 1761–1786, 2023.

[16] V. Pattanaik, B. K. Malika, P. K. Rout, and B. K. Sahu, "Contingency-resilient PMU placement using fuzzy logic and discrete artificial bee colony algorithm for comprehensive network observability," *e-Prime – Advances in Electrical Engineering, Electronics and Energy*, vol. 5, p. 100275, 2023.

[17] A. R. Jordehi*et al.*, "Optimal placement of hydrogen fuel stations in power systems with high photovoltaic penetration and responsive electric demands in presence of local hydrogen markets," *Int. J. Hydrogen Energy*, vol. 50, pp. 62–76, 2024.

[18] A. K. Mohanty and S. B. Perli, "Fuzzy logic based multi-objective approach for optimal allocation of charging stations for electric vehicles," *e-Prime – Advances in Electrical Engineering, Electronics and Energy*, vol. 2, p. 100089, 2022.

[19] I. Ziari and A. Jalilian, "A new approach for allocation and sizing of multiple active power-line conditioners," *IEEE Trans. Power Del.*, vol. 25, no. 2, pp. 1026–1035, 2010.

[20] M. Farhoodnea, A. Mohamed, H. Shareef, and H. Zayandehroodi, "Optimum placement of active power conditioner in distribution systems using improved discrete firefly algorithm for power quality enhancement," *Appl. Soft Comput.*, vol. 23, pp. 249–258, 2014.

[21] A. Lakum and V. Mahajan, "Optimal placement and sizing of multiple active power filters in radial distribution system using grey wolf optimizer in presence of nonlinear distributed generation," *Electr. Power Syst. Res.*, vol. 173, pp. 281–290, 2019.

[22] A. Lakum, D. Bhonsle, and M. Pandya, "Optimal placement and sizing of active power filters in RDS using TLBO for harmonic distortion reduction," in *Int. Online Conf. Smart Grid Energy Syst. Control*, Springer, 2023.

[23] D. H. Wolpert and W. G. Macready, "No free lunch theorems for optimization," *IEEE Trans. Evol. Comput.*, vol. 1, no. 1, pp. 67–82, 1997.

[24] X.-S. Yang, "A new metaheuristic bat-inspired algorithm," in *Nature Inspired Cooperative Strategies for Optimization (NICSO 2010)*, Springer, 2010, pp. 65–74.

[25] X.-S. Yang and X. He, "Bat algorithm: literature review and applications," *Int. J. Bio-Inspired Comput.*, vol. 5, no. 3, pp. 141–149, 2013.

[26] A. T. Olusesi*et al.*, "Energy management model for mobile ad hoc network using adaptive information weight bat algorithm," *e-Prime – Advances in Electrical Engineering, Electronics and Energy*, vol. 5, p. 100255, 2023.

[27] J. W. Zhang and G. G. Wang, "Image matching using a bat algorithm with mutation," *Appl. Mech. Mater.*, vol. 203, pp. 88–93, 2012.

[28] S. Mishra, K. Shaw, and D. Mishra, "A new meta-heuristic bat inspired classification approach for microarray data," *Procedia Technol.*, vol. 4, pp. 802–806, 2012.

[29] P. Musikapun and P. Pongcharoen, "Solving multi-stage multi-machine multi-product scheduling problem using bat algorithm," in *Proc. 2nd Int. Conf. Manag. Artif. Intell.*, IACSIT Press, Singapore, 2012.

[30] O. Maroufi, A. Choucha, and L. Chaib, "Hybrid fractional fuzzy PID design for MPPT-pitch control of wind turbine-based bat algorithm," *Electr. Eng.*, vol. 102, no. 4, pp. 2149–2160, 2020.

[31] T. Niknam, S. Sharifinia, and R. Azizipanah-Abarghooee, "A new enhanced bat-inspired algorithm for finding linear supply function equilibrium of GENCOs in the competitive electricity market," *Energy Convers. Manag.*, vol. 76, pp. 1015–1028, 2013.

[32] S. S. Reddy, "Bat algorithm-based back propagation approach for short-term load forecasting considering weather factors," *Electr. Eng.*, vol. 100, no. 3, pp. 1297–1303, 2018.

[33] F. C. Sampaio*et al.*, "Adaptive fuzzy directional bat algorithm for the optimal coordination of protection systems based on directional overcurrent relays," *Electr. Power Syst. Res.*, vol. 211, p. 108619, 2022.

[34] D. Sambariya and R. Prasad, "Robust tuning of power system stabilizer for small signal stability enhancement using metaheuristic bat algorithm," *Int. J. Electr. Power Energy Syst.*, vol. 61, pp. 229–238, 2014.

[35] X.-S. Yang, *Nature-Inspired Metaheuristic Algorithms*, Luniver Press, 2010.

[36] J. D. Altringham, *Bats: Biology and Behaviour*, Oxford Univ. Press, 1996.

[37] X.-B. Meng, X. Z. Gao, Y. Liu, and H. Zhang, "A novel bat algorithm with habitat selection and Doppler effect in echoes for optimization," *Expert Syst. Appl.*, vol. 42, no. 17–18, pp. 6350–6364, 2015.

[38] X. Cao, C. Wang, and W. Li, "A novel bat algorithm with asymmetrical weighed variational method in the path planning of UAVs," *Symmetry*, vol. 15, no. 6, p. 1265, 2023.

[39] X. Liu, W. Peng, L. Xie, and X. Zhang, "Optimization of a multi-type PMSM based on pyramid neural network," *Appl. Sci.*, vol. 13, no. 11, p. 6810, 2023.

[40] E. De Oliveira *et al.*, "Efficient hybrid algorithm for transmission expansion planning," *Electr. Eng.*, vol. 100, pp. 2765–2777, 2018.

International Journal of
Electrical and Electronics Research (IJEER)
Research Article | Volume 14, Issue 2 | Pages 279-289 | e-ISSN: 2347-470X

[41] K. Guerraiche, L. Dekhici, E. Chatelet, and A. Zeblah, "Multi-objective electrical power system design optimization using a modified bat algorithm," *Energies*, vol. 14, no. 13, p. 3956, 2021.

[42] J.-H. Teng and C.-Y. Chang, "Backward/forward sweep-based harmonic analysis method for distribution systems," *IEEE Trans. Power Del.*, vol. 22, no. 3, pp. 1665–1672, 2007.

[43] M. Shivaie, A. Salemnia, and M. T. Ameli, "Optimal multi-objective placement and sizing of passive and active power filters by a fuzzy-improved harmony search algorithm," *Int. Trans. Electr. Energy Syst.*, vol. 25, no. 3, pp. 520–546, 2013.

[44] S. Sakar, M. E. Balci, S. H. A. Aleem, and A. F. Zobaa, "Increasing PV hosting capacity in distorted distribution systems using passive harmonic filtering," *Electr. Power Syst. Res.*, vol. 148, pp. 74–86, 2017.

[45] S. Sakar, M. E. Balci, S. H. A. Aleem, and A. F. Zobaa, "Integration of large-scale PV plants in non-sinusoidal environments: Considerations on hosting capacity and harmonic distortion limits," *Renew. Sustain. Energy Rev.*, vol. 82, pp. 176–186, 2018.

[46] J.-H. Teng, S.-H. Liao, and R.-C. Leou, "Three-phase harmonic analysis method for unbalanced distribution systems," *Energies*, vol. 7, no. 1, pp. 365–384, 2014.

[47] J. Savier and D. Das, "Impact of network reconfiguration on loss allocation of radial distribution systems," *IEEE Trans. Power Del.*, vol. 22, no. 4, pp. 2473–2480, 2007.

[48] E. Fuchs and M. A. Masoum, *Power Quality in Power Systems and Electrical Machines*, Academic Press, 2011.

[49] A. R. Oliva and J. C. Balda, "A PV dispersed generator: a power quality analysis within the IEEE 519," *IEEE Trans. Power Del.*, vol. 18, no. 2, pp. 525–530, 2003.